Journal of Alloys and Compounds 627 (2015) 192–199

Contents lists available at ScienceDirect

Journal of Alloys and Compounds

journal homepage: www.elsevier.com/locate/jalcom

Development of high performance magnesium composites using $Ni_{50}Ti_{50}$ metallic glass reinforcement and microwave sintering approach

S. Sankaranarayanan [a], V. Hemanth Shankar [b], S. Jayalakshmi [a,c], Nguyen Quy Bau [a], Manoj Gupta [a,*]

[a] Department of Mechanical Engineering, National University of Singapore, 9 Engineering Drive 1, Singapore 117576, Singapore
[b] Department of Metallurgical and Materials Engineering, National Institute of Technology, Tiruchirappalli, Tamil Nadu 620015, India
[c] Department of Mechanical Engineering, Bannari Amman Institute of Technology, Satyamangalam, Tamil Nadu 638 401, India

ARTICLE INFO

Article history:
Received 29 October 2014
Accepted 3 December 2014
Available online 12 December 2014

Keywords:
Magnesium
Amorphous alloy reinforcements
Microwave sintering
Structural properties
Mechanical properties

ABSTRACT

The present study illustrates the structural and mechanical properties of magnesium composites containing $Ni_{50}Ti_{50}$ metallic glass reinforcement particles. Novel Mg-composites containing 3, 6 and 10 vol.%$Ni_{50}Ti_{50}$ amorphous particulates were synthesized using the microwave assisted rapid sintering technique followed by hot extrusion. The developed Mg-composite materials were investigated for their microstructural and mechanical properties. Microstructural studies revealed the retention of amorphous structure of $Ni_{50}Ti_{50}$ reinforcement and its fair distribution in developed Mg/$Ni_{50}Ti_{50}$ composites. Mechanical property evaluation under indentation and compression loads showed significant enhancement in strength properties (microhardness:+78%, 0.2CYS:+79%, UCS:+70%, 0.2TYS:+95%, UTS:+50%) without compromising the compressive ductility. For the first time, tensile properties of such amorphous particles reinforced Mg-composites were studied and the results showed ~98% increase in 0.2TYS and ~50% increase in UTS. The tensile ductility was adversely affected. However, the obtained values are comparable to that of conventional Mg-composites. The observed mechanical response discussed in terms of structure–property relationship highlights the efficacy of amorphous $Ni_{50}Ti_{50}$ reinforcement particles and the energy efficient microwave sintering approach to produce high performance magnesium composites.

1. Introduction

In recent years, automotive and aircraft manufacturers are investing in great deal into the research and development of light weight, energy efficient magnesium based materials [1–3]. Besides being the lightest structural metal with density only slightly greater than plastics, magnesium (Mg) also possess notable properties such as excellent damping capacity, castability, machinability, and low temperature processing advantages which makes it suitable for a spectrum of engineering applications [4]. In spite, the commercial use of Mg is rather restricted due to its inherent mechanical characteristics such as low elastic modulus, low strength and poor high temperature stability [4]. Literature study reveals that most of these limitations can be circumvented through the judicious incorporation of alloying elements and/or reinforcements. Conventionally, alloying elements such as Al, Zn and Zr are added to Mg to develop Mg-alloys with improved mechanical properties [1–4]. However, most Mg-alloys exhibit poor thermal stability and to overcome this, high strength, high modulus ceramic reinforcement are often introduced into pure Mg and its alloys to produce Mg-metal matrix composites (Mg-MMCs) [5]. While the Mg-MMCs are known to exhibit high thermal stability alongside strength, modulus, and wear resistance, they suffer from extreme brittleness due to interfacial de-cohesion and undesirable reactions at (ceramic) particle – (metallic) matrix interface [6]. In this regard, the role of metallic reinforcement addition to pure Mg and Mg-alloys has been investigated by various researchers [7–9] and the introduction of such metallic reinforcements in these studies has positively influenced the overall mechanical response of Mg-materials.

Metallic glasses are novel metallic materials that exhibit superior properties such as high strength, hardness and elastic strain limit etc. Recently, there have been some attempts to use the metallic glass particles as reinforcement in metal matrix composites [10,11]. A study of available open literature shows that the investigations on amorphous alloy incorporation in Mg-matrices are still in the early stage as only limited studies have been successfully carried out so far. Dudina et al. [10] developed AZ91 magnesium alloy matrix composite containing 15 vol.%$Zr_{57}Nb_5Cu_{15.4}Ni_{12.6}Al_{10}$ amorphous powder (produced by milling of melt spun amorphous ribbon). The mechanical properties of composite studied under indentation and compression revealed a remarkable ~125%

* Corresponding author. Tel.: +65 6516 6358.
E-mail address: mpegm@nus.edu.sg (M. Gupta).

http://dx.doi.org/10.1016/j.jallcom.2014.12.009
0925-8388/

enhancement in compressive yield strength and ~80% enhancement in hardness. In our recent research work [11], we have studied the hardness and compressive properties of $Ni_{60}Nb_{40}$ amorphous particle reinforced Mg composite synthesized using microwave assisted rapid sintering technique, which is an energy conservative method employing two-directional heating to sinter powder compacts (i.e. through a combined action of microwaves and microwave-coupled external heating source), as high sintering temperatures (closer to the melting point) can be achieved in a relatively shorter period of time allowing energy and time savings [12]. Microstructural characterization in this study [11] showed that the amorphous structure of reinforcements can be retained through the proper selection of microwave heating time and the mechanical testing results showed ~120% improvement in Vickers hardness and ~85% increase in compressive strength.

With this background, the current research work is aimed at the development of new Mg-MMCs containing Ni–Ti based $Ni_{50}Ti_{50}$ metallic glass particles through the bidirectional microwave sintering assisted powder metallurgy method. The $Ni_{50}Ti_{50}$ metallic glass particles required for this study were synthesized using mechanical alloying and then incorporated into pure Mg matrix using the blend-press-sinter based powder metallurgy technique followed by hot extrusion. The hot extruded Mg-composites were investigated for their structural and mechanical properties. Structure–property relationships were invoked in order to comprehend the properties exhibited by the developed composites.

2. Experimental procedures

2.1. Preparation of amorphous reinforcement

The preparation of $Ni_{50}Ti_{50}$ (in atomic percent, at.%) amorphous powder involves mechanical alloying of elemental Ni (***Size***: 40 μm, ***Purity***: 99.9%, ***Supplier***: Alfa Aesar, USA) and Ti (***Size***:<140 μm, ***Purity***: 99.9%, ***Supplier***: Merck, Germany) metal powder in a Retsch PM400 planetary ball-milling machine using a ball-to-powder ratio of 3:1 and milling speed of 200 rpm.

2.2. Preparation of magnesium–metal matrix composites

In the next step, pure Mg powder (***Size***: 60–300 μm, ***Purtiy***: 99%, ***Supplier***: Merck, Germany) was mixed with different amounts (3 vol.%, 6 vol.% and 10 vol.%) of amorphous $Ni_{50}Ti_{50}$ powder in a RETSCH PM-400 mechanical alloying machine at 200 rpm for 1 h. No balls or process control agent was used in this stage. The blended powder mixture is then cold-pressed at the pressure of 50 tons into billets of size 35 mm diameter and 40 mm length. The compacted billets were then subjected to rapid sintering in a 900 W, 2.45 GHz Sharp microwave oven for 11 min. The sintered billets were coated with colloidal graphite and soaked at 400 °C for 1 h, and hot extruded at 400 °C to obtain rods of 8 mm in diameter. Samples from the extruded rods were used for further characterization.

2.3. Property characterization

2.3.1. Structural properties

Structural properties of the reinforcement powder and the bulk Mg-composites were studied using a Shimadzu LAB-XRD-6000 (Cu Kα; λ = 1.54056 A°) spectrometer, an Olympus optical microscope and a Hitachi FESEM-S4300 coupled with energy dispersion (EDS) analyzer. In order to identify the structural changes during ball-milling process, the powder samples of the as-received Ni, Ti and the ball-milled $Ni_{50}Ti_{50}$ were subjected to X-ray and SEM analyses. The characteristics of bulk Mg-composites developed in this study were studied in terms of the average matrix grain size, the distribution and nature of reinforcement particles/s phases. For this purpose, microstructural analyses were carried out on the metallographic specimens prepared from the extruded rod which involved grinding and polishing. The surface of the polished samples was then etched with citral (4.2 g of citric acid monohydrate in 100 ml of water) to reveal the grain boundaries and observed in optical/scanning electron microscopy to identify the grain size and morphology. From selected optical/SEM micrographs, the area of each grain and hence the diameter of each grain were obtained using the Scion Image software. A total of 120–150 grains were selected to calculate the grain characteristics.

2.3.2. Mechanical properties

Mechanical properties of the developed Mg-MMCs under indentation, compression and tension loading were measured in accordance with standard test methods. Microhardness measurements were performed on the polished samples using a Matsuzawa MXT 50 automatic digital microhardness tester. The microhardness test was performed using a Vickers indenter under a test load of 25 gf and a dwell time of 15 s in accordance with ASTM: E384-11e1. The compressive and tensile properties of the as extruded pure magnesium and its composite counterparts were determined using an MTS 810 automated servo hydraulic mechanical testing machine in accordance with the procedures outlined in ASTM standards E9-09 and E8/E8M-13a respectively. The crosshead speed was set at 4×10^{-7} m/s (strain rate: 0.010 min^{-1}) and 6.67×10^{-7} m/s (strain rate: 0.005 min^{-1}) respectively. For each composition, a minimum of 6 tests were conducted to obtain repeatable values. The fractured samples were then studied using a Hitachi S-4300 FESEM to identify the fracture mechanisms.

3. Results and discussion

3.1. Fabrication of Mg/$Ni_{50}Ti_{50}$ composites

The X-ray diffractograms of the $Ni_{50}Ti_{50}$ powder after different ball-milling duration are shown in Fig. 1. It indicates that the intensity of peaks related to Ti, Ni crystalline phases decay with the milling duration and a diffused halo, typical of amorphous materials (indicating the short range order) was observed after 55 h [11]. The microstructural characteristics of the as-received Ni, Ti and the ball-milled $Ni_{50}Ti_{50}$ powder are presented in Fig. 2(a–c). It shows that the ball-milled $Ni_{50}Ti_{50}$ powder particles are mostly rounded (without sharp corners) and have irregular size ranging between 10 μm and 40 μm (Fig. 2c), which is relatively smaller when compared to that of the as-received Ni (40 μm) (Fig. 2a) and Ti (<140 μm) (Fig. 2b). This can be attributed to the fact that the ball-milling process involves repeated loading, flattening and breaking down of the powder particles [13].

The X-ray diffractograms of pure Mg and its composite containing $Ni_{50}Ti_{50}$ amorphous particles are shown in Fig. 3. It reveals prominent Mg-crystalline peaks in all the cases without any peaks corresponding to the reaction products being formed between the Mg-matrix and the amorphous reinforcement. Further, the XRD pattern of the developed composites also shows amorphous halo

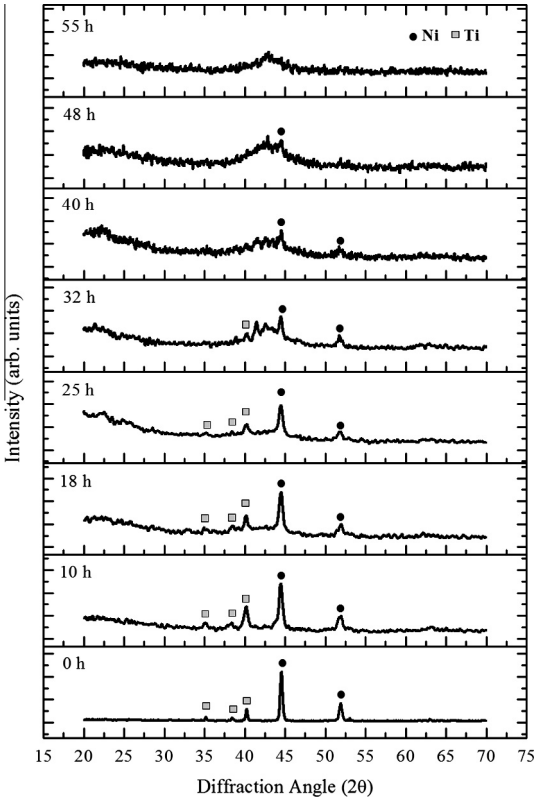

Fig. 1. X-ray diffraction pattern of $Ni_{50}Ti_{50}$ powder after different ball-milling duration.

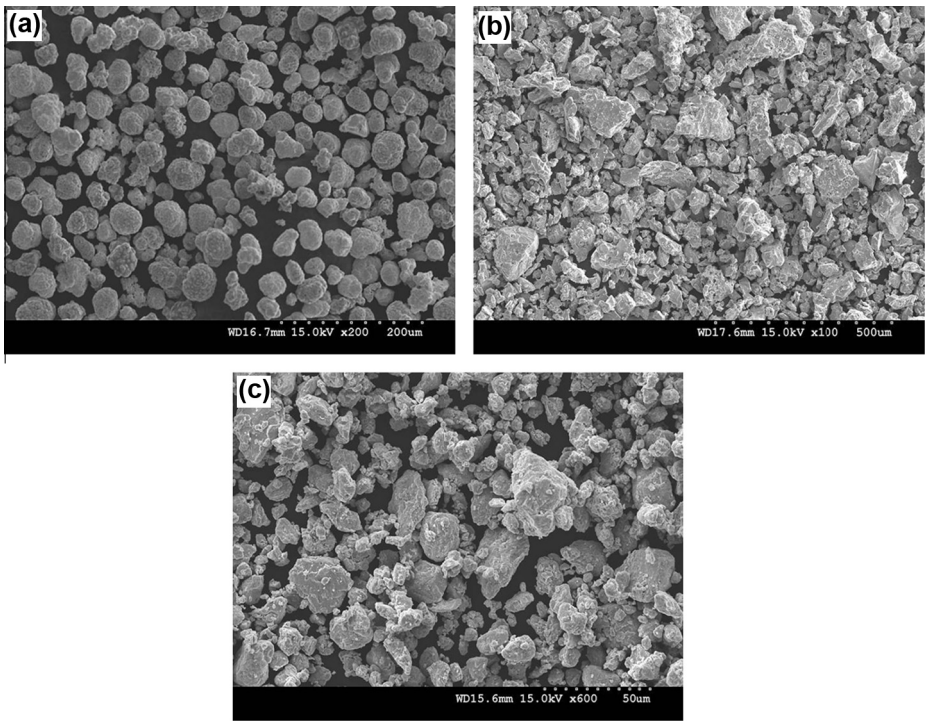

Fig. 2. SEM Micrographs of the (a) as-received Ni, (b) Ti and (c) the ball-milled $Ni_{50}Ti_{50}$ powder.

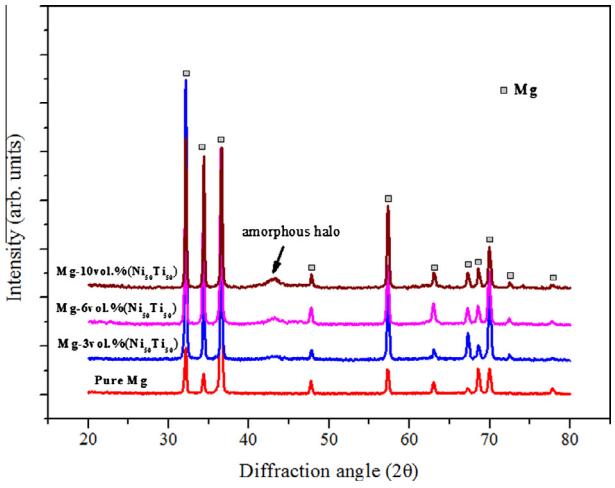

Fig. 3. X-ray diffractograms of the developed Mg-materials.

between diffraction angle $2\theta = 40°$ and 50°, thus indicating the retention of reinforcement' amorphous structure in the developed Mg-composites. These observations also confirm that the novel glassy metallic particles can be effectively incorporated into Mg matrix by using rapid microwave sintering assisted powder metallurgy process, without any significant changes to their amorphous structure, as recently reported in our article on Ni–Nb amorphous particle reinforced Mg composites [11].

3.2. Microstructure

The SEM micrographs representing the microstructural characteristics of pure Mg and Mg/x–$Ni_{50}Ti_{50}$ composites are presented in Fig. 4(a–e). Image analysis in terms of average grain size and aspect ratio, performed on these optical micrographs (Fig. 4(a–d) and Table 1) clearly exemplifies that the matrix microstructure in all the composites are composed of relatively fine and equiaxed grains when compared to pure Mg. This could well be attributed to the fact that during hot extrusion, the hard and strong amorphous $Ni_{50}Ti_{50}$ reinforcement particles present in the Mg-matrix would act as heterogeneous grain nucleation sites to generate a large number of dislocations and sub-grain boundaries (low mis-orientation angle) within the parent matrix [14,15]. Upon continuous accretion, the mis-orientation angle between the sub-grain structures amplify and devlops into high angle grain boundaries, thus resulting in matrix grain refinement and equiaxed microstructure as seen in the micrographs, Fig. 4(a–d) [15]. Among the developed composites, a significant grain refinement by ~60% was achieved in case of 6 vol.%$Ni_{50}Ti_{50}$ addition.

Regarding the distribution of amorphous $Ni_{50}Ti_{50}$ particles in the developed Mg-composites, the SEM micrographs (Fig. 4(b–d)) reveals that at all volume fractions, the $Ni_{50}Ti_{50}$ amorphous particles are fairly distributed throughout the Mg-matrix with minimal clustering or agglomeration. Available literature on wrought (extruded) Mg-MMCs reveals that the homogeneous distribution of reinforcement particles can be achieved by critically fine tuning the extrusion parameters (ratio and temperature) [16]. Hence, the microstructural characterization results' suggest that the use of process variables (extrusion ratio: 22.5:1 and temperature 400 °C) has facilitated the fairly uniform distribution of amorphous reinforcement particles in the Mg-matrix. However, micrographs corresponding to 6 and 10 vol.%$Ni_{50}Ti_{50}$ amorphous particle addition have shown clusters and the presence of such clusters in powder metallurgy processed Mg-composites have been widely reported in the available literature [11,17,18]. In these studies, it has been observed that at high volume percent reinforcement addition, the inter-particle spacing between the reinforcement particles were reduced and the particle–particle interaction becomes unavoidable, thus resulting in particle clustering or agglomeration. Further, the high energy ball-milling process used to prepare the amorphous reinforcement would also facilitate particle–particle interaction,

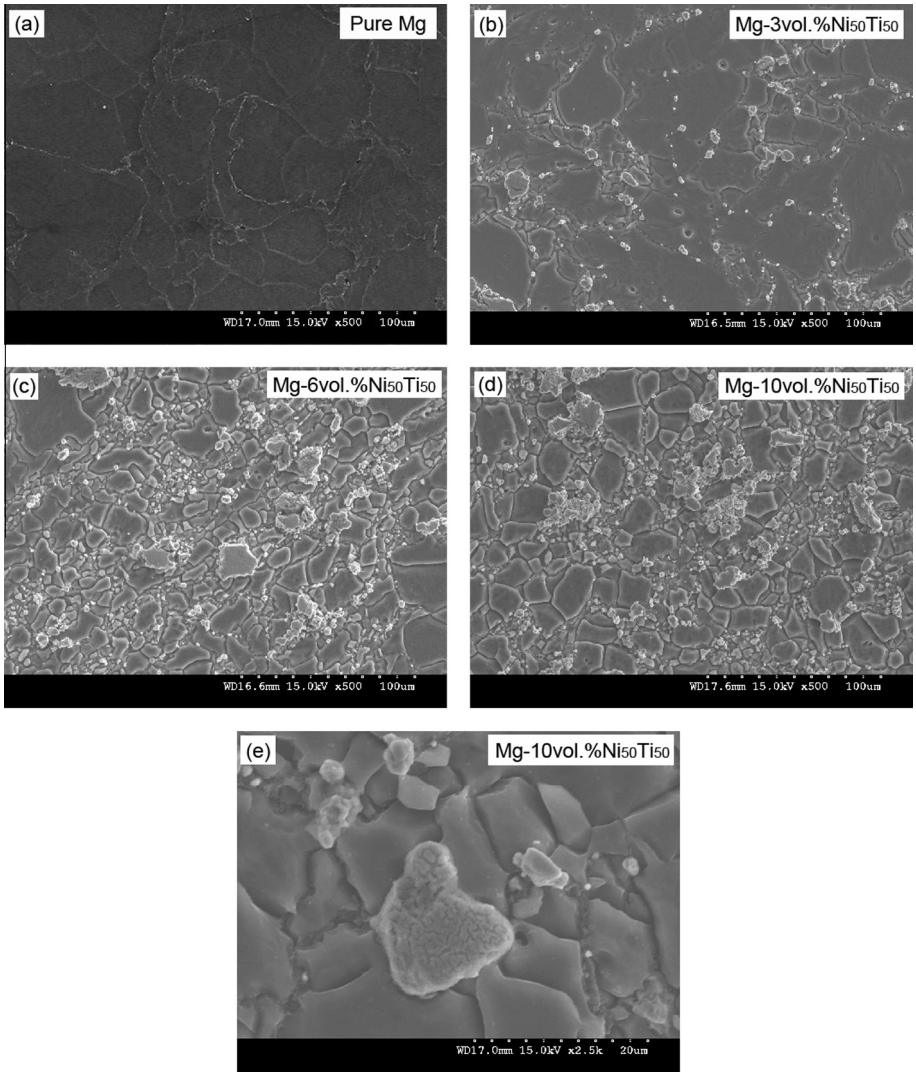

Fig. 4. SEM Micrographs showing the microstructural characteristics of (a) pure Mg, (b) Mg–3 vol.%$Ni_{50}Ti_{50}$, (c) Mg–6 vol.%$Ni_{50}Ti_{50}$, and (d) Mg–10 vol.%$Ni_{50}Ti_{50}$. (e) particle–matrix interfacial characteristics of Mg–10 vol.%$Ni_{50}Ti_{50}$.

Table 1
Results of microstructure studies.

S. No.	Material	Grain size[a] (μm)
1	Pure Mg	32 ± 7
2	Mg–3 vol.%$Ni_{50}Ti_{50}$	24 ± 12
3	Mg–6 vol.%$Ni_{50}Ti_{50}$	12 ± 6
4	Mg–10 vol.%$Ni_{50}Ti_{50}$	18 ± 4

[a] Based on approximately 80 grains.

thus resulting in enhanced clustering effects [13,19]. Fig. 4e indicates good bonding characteristics at the particle/matrix interface which can be attributed to the nature of $Ni_{50}Ti_{50}$ amorphous reinforcement.

3.3. Mechanical properties

The results of microhardness measurements conducted on pure Mg and its composites containing $N_{i50}Ti_{50}$ amorphous reinforcement are shown in Table 2. It indicates that the incorporation of $Ni_{50}Ti_{50}$ amorphous particles has significantly improved the indentation resistance of pure Mg. Table 2 also shows that the increment in microhardness trend follows closely with the amount of amorphous reinforcement and a maximum enhancement by ~106% was obtained in case of Mg–10 vol.%$Ni_{50}Ti_{50}$ composite. The observed increase in microhardness can hence be attributed to the matrix work-hardening effects (constraint to localized matrix deformation) offered by the inherent hard and strong (860 ± 31 H_v, measured) amorphous $Ni_{50}Ti_{50}$ reinforcement particles during indentation. Table 2 also shows that the noticeable enhancement in indentation resistance obtained in the developed composites are superior compared to Mg-ceramic composites and similar to metallic (armorphous) particle reinforced Mg-composites [7,8,20,21].

The compressive properties of pure Mg and its composites reinforced with $Ni_{50}Ti_{50}$ amorphous particles are listed in Table 3 and shown in Fig. 5. Table 3 also lists the properties of various conventional ceramic particle reinforced Mg–metal matrix composites. From the test results (Table 3, Fig. 5), it can be seen that the $Ni_{50}Ti_{50}$ amorphous particle reinforced Mg composites showed excellent improvement in both the 0.2% offset compressive yield strength (0.2%CYS) and ultimate compressive strength (UCS) without largely affecting the compressive ductility. While an increase in 0.2%CYS and UCS by ~15% and ~25% respectively, was seen in case of 3 vol.%$Ni_{50}Ti_{50}$ particle addition, the Mg–10 vol.%$Ni_{50}Ti_{50}$ composite containing highest reinforcement volume fraction (10 vol.%) showed a remarkable enhancement in

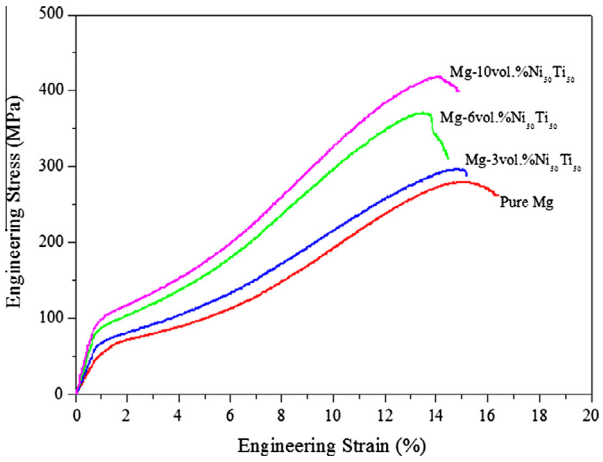

Fig. 5. Engineering stress–strain curves of the developed Mg-composites under compressive loading.

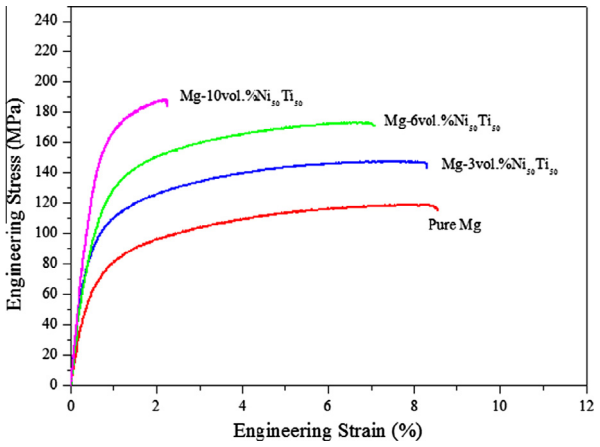

Fig. 7. Engineering stress–strain curves of the developed Mg-composites under tensile loading.

0.2%CYS and UCS by ~79% and ~71% respectively. In case of compressive ductility, all the composite samples developed in this study showed similar values which are slightly inferior to that of pure Mg. However, considering standard deviation, it can be seen that the compressive ductility of Mg remained largely unchanged after $Ni_{50}Ti_{50}$ amorphous particle addition. This is unlike other Mg-MMCs which often showed poor ductility upon the incorporation of ceramic reinforcement, which could well be attributed to the inherent high elastic strain of the amorphous particles and thus highlighting its beneficial role as novel reinforcement [21–23]. Table 3 also show that the incorporation of amorphous-$Ni_{50}Ti_{50}$ particles has strongly (positively) influenced the ultimate compressive strength of the developed Mg-composites which is unlike those observed in Mg/Ni60Nb40 composites developed through similar processing method. Further, it is also interesting to note that the developed Mg/$Ni_{50}Ti_{50}$ composites have exhibited excellent overall compressive response which is mostly superior to other Mg-composites reinforced with conventional ceramic or metallic reinforcement as listed in Table 3.

Further, the compressive flow curves (Fig. 5) also clearly show that the crystallographic orientation has largely influenced the compressive deformation of the developed Mg-composites. The sigmoidal nature with high work hardening behavior indicates that the compressive deformation has occurred by the (tensile) twinning process [24]. The representative fractographic images of the compression failed samples, Fig. 6(a and b) clearly show shear mode fracture in both pure Mg and its composite developed in this study which also confirms that the compressive deformation of the developed Mg-composites is significantly indifferent.

The results of tensile property measurements conducted on the developed Mg-composites containing amorphous reinforcement under tensile loading are listed in Table 4. It also lists the tensile properties of few conventional Mg-MMCs. Fig. 7 shows the representative engineering stress–strain curves of the developed Mg-composites under tensile loads. The results indicate that significant enhancement in 0.2%TYS (Tensile yield strength) and UTS (Ultimate tensile strength) of Mg were obtained due to $Ni_{50}Ti_{50}$ amorphous reinforcement addition. In this study, the strength properties increment trend due to $Ni_{50}Ti_{50}$ amorphous particle addition follows increasing reinforcement volume percent. When compared to pure Mg, the developed Mg–10 vol.%$Ni_{50}Ti_{50}$ composite containing larger volume percent reinforcement showed ~98% and ~50% enhancement in 0.2% TYS (from 75 MPa to 148 MPa) and UTS (from 119 MPa to 178 MPa) values. In case of ductility, a decreasing trend was observed with increasing volume percent of amorphous particle incorporation. However, the overall tensile properties of the developed Mg/$Ni_{50}Ti_{50}$ are mostly superior to that seen in case of conventional MMCs [7,8,20,23].

The microscopic features of tension test failed samples of pure-Mg and the $N_{i50}Ti_{50}$ particle reinforced Mg-composites are shown in Fig. 8. The observed microscopic fracture features in Fig. 8(a and b) are indicative of quasi-cleavage fracture in pure Mg and its composites reinforced with amorphous $Ni_{50}Ti_{50}$ particles. In addition, particle segregation (debonding) features (Fig. 8c) were also prominently seen in the composites containing larger volume percent of reinforcement particles. In the absence of any interfacial reaction products with good bonding characteristics (structural coherency) at the particle matrix interface, particle debonding or segregation is expected once the maximum load transfer from

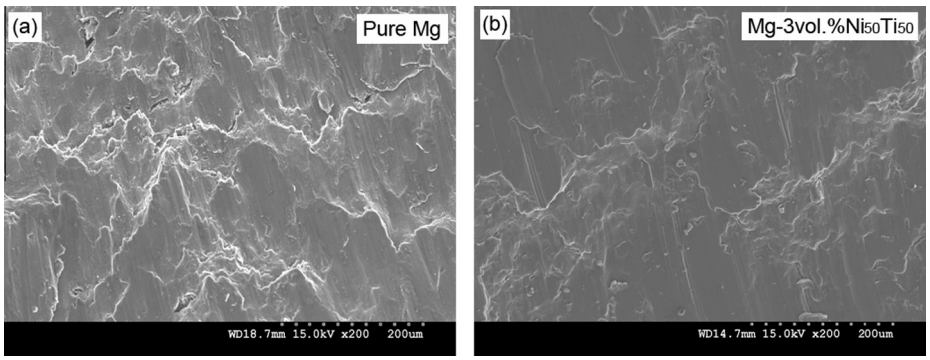

Fig. 6. Representative compressive fracture surfaces showing shear bands in (a) pure Mg and (b) Mg–3 vol.%$Ni_{50}Ti_{50}$.

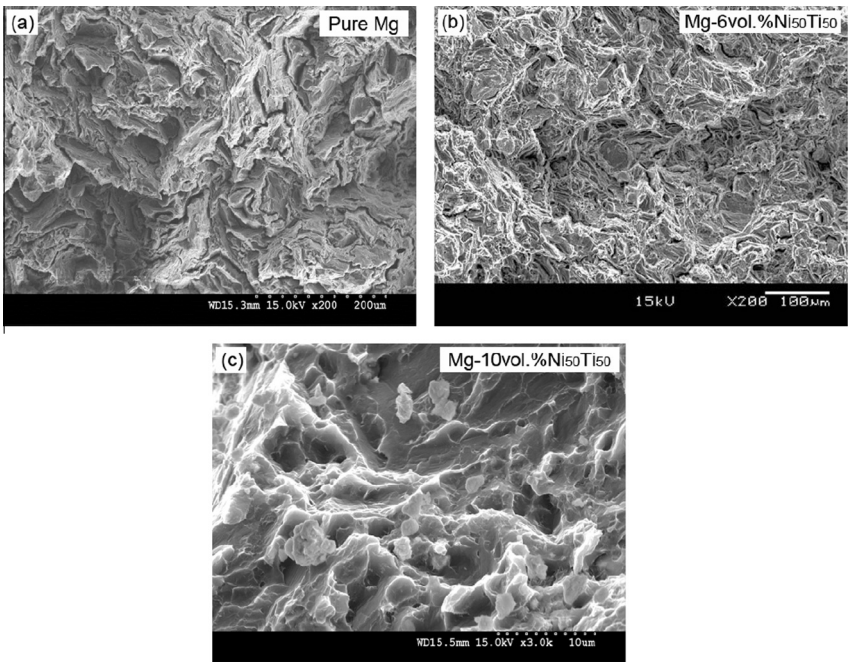

Fig. 8. Representative tensile fractographs showing typical cleavage mode fracture in (a) pure Mg and (b) Mg–6 vol.%$Ni_{50}Ti_{50}$ and (c) prominent particle segregation in Mg–10 vol.%$Ni_{50}Ti_{50}$.

Table 2
Results of microhardness measurements.

S. No.	Material	Microhardness (Hv)	Percentage increase in hardness with respect to pure Mg
1	Pure Mg	32 ± 6	
2	Mg–3 vol.%$Ni_{50}Ti_{50}$	49 ± 3	53%
3	Mg–6 vol.%$Ni_{50}Ti_{50}$	62 ± 4	95%
4	Mg–10 vol.%$Ni_{50}Ti_{50}$	66 ± 8	106%
5	Pure Mg [11]	43 ± 2	
	Mg–3 vol.%$Ni_{60}Nb_{40}$ [11]	62 ± 4	44%
	Mg–5 vol.%$Ni_{60}Nb_{40}$ [11]	84 ± 5	95%
	Mg–10 vol.%$Ni_{60}Nb_{40}$ [11]	95 ± 5	120%
6	Mg (cast) [10]	68	
	Mg–15 vol.% $Zr_{57}Nb_5Cu_{15.4}Ni_{12.6}Al_{10}$ (cast) [10]	123	81%
7	Mg [20]	39.7 ± 1.6	
	Mg–9.3 vol.%SiC [20]	42.9 ± 5.8	8%
	Mg–12.8 vol.%SiC [20]	43.0 ± 1.0	8%
8	Mg [21]	50	
	Mg–5 vol.%Y_2O_3 [21]	56	12%
9	Pure Mg [9]	48 ± 1	47%
	Mg–2.2 vol.%Ti [9]	71 ± 2	

the matrix to reinforcement is reached (UTS). Hence, the developed composite formulations showed particle debonding features.

The strength properties improvement due to $N_{i50}Ti_{50}$ amorphous reinforcement addition under micro-indentation, compression and tension loads can be attributed to the following factors: (i) ***Load bearing effect***: The inherent superior strength and hardness of the amorphous reinforcement (860 ± 31 H_v, measured) is expected to improve the strength of Mg by efficient load sharing/transfer from the soft Mg-matrix to the hard and strong reinforcement particles [25]. Available literature suggests that strong interfacial bonding between the matrix and reinforcement can be achieved by minimizing the brittle reaction between the matrix and reinforcement phases. Hence, the strength enhancement obtained in this study (Tables 2–4) could well be attributed to the good/clear interfacial bonding characteristics between the Mg-matrix and amorphous reinforcement, as seen in Fig. 4e. (ii) ***Dislocation generation and interaction***: The mismatch in elastic modulus and thermal expansion coefficients between the Mg-matrix ($\alpha_{Mg} = 28.9 \times 10^{-6}\ K^{-1}$, $G_{Mg} = 17.3$ GPa) and reinforcements ($\alpha_{Ni(A)} = 14.2 \times 10^{-6}\ K^{-1}$, $G_{Ni(A)} = >100$ GPa) would result in the introduction of mechanical/thermal residual stress in the composites [25–29]. In turn, the residual stress would increase the dislocation density at the particle/matrix interface and hence contribute to the strength properties improvement and plastic deformation [25,29]. (iii) ***Grain size strengthening***: The increase in grain boundary area due to reduction in grain size (grain refinement) would also impede the movement of dislocations and contribute toward an increase in dislocation density [25,29] which will result in the onset of plastic deformation and improves the yield strength.

The mechanical testing results' also clearly highlights that the properties of the developed Mg-composites were greatly influenced by the amount and distribution of reinforcement particles in the Mg-matrix. Especially, in case of Mg–10 vol.%$Ni_{50}Ti_{50}$ composite, wherein the relatively larger reinforcement volume has remarkably enhanced the strength under both tension and compression, however with adverse effects on the tensile ductility. This could be because of the reduced inter-particle spacing between the reinforcement particles at larger volume of reinforcement addition [30,31]. It is known that the reduced reinforcement particle spacing would generally increase the residual stress at particle–matrix interface, and under tensile loads, in the absence of strong chemical bond between the matrix and reinforcement (no intermetallics with strong bond at Mg/reinforcement interface), the reduced inter-particle spacing and the residual stresses at particle–matrix interface would ease the linking of particle–matrix interfacial cracks and particle segregation/debonding (as particle–matrix bonding is largely controlled by the particles' stress state) to result in premature failure [30–32]. However, this is relatively uncommon under compressive loads. Hence, the compressive ductility of the developed composites was largely unaffected which could also be attributed to the unique properties of high strength and high elastic strain limit (~2%) of the amorphous particles.

Table 3
Results of room temperature compression testing.

S. No.	Material	0.2 Compressive yield strength (MPa)	Ultimate compressive strength (MPa)	Failure strain (%)
1	Pure Mg	58 ± 8	234 ± 8	16.4 ± 0.9
2	Mg–3 vol.%$Ni_{50}Ti_{50}$	67 ± 9 (15%)	291 ± 12 (25%)	15.9 ± 0.7
3	Mg–6 vol.%$Ni_{50}Ti_{50}$	89 ± 3 (54%)	368 ± 8 (57%)	15.1 ± 1.5
4	Mg–10 vol.%$Ni_{50}Ti_{50}$	102 ± 4 (79%)	417 ± 6 (70%)	14.9 ± 2.0
5	Pure Mg [11]	70 ± 6	265 ± 8	16.2 ± 0.8
	Mg–3 vol.%$Ni_{60}Nb_{40}$ [11]	85 ± 4 (21%)	283 ± 10 (6%)	17.6 ± 1.1
	Mg–5 vol.%$Ni_{60}Nb_{40}$ [11]	130 ± 11 (85%)	320 ± 11 (20%)	18.4 ± 1.3
	Mg–10 vol.%$Ni_{60}Nb_{40}$ [11]	90 ± 7 (28%)	322 ± 10 (20%)	17.2 ± 1.6
6	Mg (cast) [10]	143	–	10.5
	Mg–15 vol.%$Zr_{57}Nb_5Cu_{15.4}Ni_{12.6}Al_{10}$ (cast) [10]	325 (127%)	–	21.0
7	Mg [21]	195	240	10
	Mg–5 vol.%Y_2O_3 [21]	205 (5%)	225 (−6%)	15 (50%)
	Mg [23]	–	169	11.9
8	Mg–22 vol%Saffil [23]	–	339 (100%)	4.6 (−62%)
9	Mg [22]	74 ± 3	273 ± 11	22.7 ± 4.9
	Mg–2.2 vol.%Ti [22]	85 ± 3 (15%)	360 ± 5 (32%)	13.6 ± 1.2 (−41%)

Numbers in bracket shows percentage improvement when compared to pure Mg.

Table 4
Results of room temperature tensile testing.

S. No.	Material	0.2 Tensile yield strength (MPa)	Ultimate tensile strength (MPa)	Failure strain (%)
1	Pure Mg	75 ± 9	119 ± 11	8.6 ± 2.1
2	Mg–3 vol.%$Ni_{50}Ti_{50}$	94 ± 5 (25%)	144 ± 6 (20%)	8.8 ± 1.7
3	Mg–6 vol.%$Ni_{50}Ti_{50}$	127 ± 4 (70%)	183 ± 6 (54%)	6.5 ± 0.9
4	Mg–10 vol.%$Ni_{50}Ti_{50}$	148 ± 7 (98%)	178 ± 9 (50%)	2.0 ± 1.3
5	Mg [20]	126 ± 14	200 ± 5	11.7 ± 3.1
	Mg–9.3 vol.%SiC [20]	120 ± 5	181 ± 6	4.7 ± 1.3
	Mg–12.8 vol.%SiC [20]	128 ± 8	176 ± 4	1.4 ± 0.1
6	Mg		91	10
	Mg–22 vol%Saffil [23]		163 (80%)	1.0

Numbers in bracket shows percentage improvement when compared to pure Mg.

4. Conclusions

In this study, novel Mg-composites containing $Ni_{50}Ti_{50}$ amorphous alloy particles were synthesized using microwave assisted rapid sintering technique, followed by hot extrusion. The developed composites were investigated for their microstructural and mechanical properties. Based on the microstructure - mechanical property correlation, the following conclusions are drawn.

1. Microwave sintering followed by hot extrusion can successfully synthesize magnesium composites containing $Ni_{50}Ti_{50}$ amorphous reinforcement without altering its amorphous structure.
2. The addition of $Ni_{50}Ti_{50}$ amorphous reinforcement significantly reduced the matrix grain size and increased the hardness when compared to pure Mg.
3. Under compressive loads, the incorporation of $Ni_{50}Ti_{50}$ amorphous particles has significantly enhanced the strength of pure Mg (by ~80%) without largely affective the ductility.
4. Under tensile loads, the developed Mg/$Ni_{50}Ti_{50}$ composites exhibit enhanced strength due to efficient load transfer and matrix strengthening. The tensile ductility was compromised with increasing amorphous reinforcement content. However, the obtained ductility values are at par/superior than that of conventional Mg-MMCs.
5. The enhancement in mechanical properties highlights beneficial role of amorphous reinforcement addition to pure Mg.

Acknowledgements

The authors wish to acknowledge the funding support given by Ministry of Education - Singapore under grant "Singapore Ministry of Education Academic Research Fund - Tier 1" and WBS No: R-265-000-493-112, for carrying out this project.

References

[1] H. Watarai, Trend of research and development for magnesium alloys, Sci. Technol. Trends 18 (2006) 84–97.
[2] A.A. Luo, Magnesium: current and potential automotive applications, Jom 54 (2002) 42–48.
[3] E. Aghion, B. Bronfin, F. Von Buch, S. Schumann, H. Friedrich, Newly developed magnesium alloys for powertrain applications, Jom 55 (2003) 30–33.
[4] M.M. Avedesian, H. Baker, ASM specialty handbook: magnesium and magnesium alloys, ASM Int. 274 (1999).
[5] I. Ibrahim, F. Mohamed, E. Lavernia, Particulate reinforced metal matrix composites—a review, J. Mater. Sci. 26 (1991) 1137–1156.
[6] Z. Zhang, B.Q. Han, D. Witkin, L. Ajdelsztajn, E.J. Laverna, Synthesis of nanocrystalline aluminum matrix composites reinforced with in situ devitrified Al–Ni–La amorphous particles, Scripta Mater. 54 (2006) 869–874.
[7] S. Hassan, M. Gupta, Development of a novel magnesium/nickel composite with improved mechanical properties, J. Alloys comp. 335 (2002) L10–L15.
[8] S. Hassan, M. Gupta, Development of a novel magnesium–copper based composite with improved mechanical properties, Mater. Res. Bull. 37 (2002) 377–389.
[9] S. Hassan, M. Gupta, Development of ductile magnesium composite materials using titanium as reinforcement, J. Alloys Comp. 345 (2002) 246–251.
[10] D. Dudina, K. Georgarakis, Y. Li, M. Aljerf, A. LeMoulec, A. Yavari, A. Inoue, A magnesium alloy matrix composite reinforced with metallic glass, Compos. Sci. Technol. 69 (2009) 2734–2736.
[11] S. Jayalakshmi, S. Sahu, S. Sankaranarayanan, S. Gupta, M. Gupta, Development of novel Mg–$Ni_{60}Nb_{40}$ amorphous particle reinforced composites with enhanced hardness and compressive response, Mater. Des. 53 (2014) 849–855.
[12] M. Gupta, W. Leong, W. Eugene, Microwave heating of metal-based materials, Microwaves Metals, 65–157.
[13] C. Suryanarayana, Mechanical alloying and milling, Prog. Mater. Sci. 46 (2001) 1–184.
[14] R. Davies, V. Randle, G. Marshall, Continuous recrystallization—related phenomena in a commercial Al–Fe–Si alloy, Acta Mater. 46 (1998) 6021–6032.
[15] F.J. Humphreys, M. Hatherly, Recrystallization and Related Annealing Phenomena, Elsevier, 1995.
[16] K. Tun, M. Gupta, Effect of extrusion ratio on microstructure and mechanical properties of microwave-sintered magnesium and Mg/Y_2O_3 nanocomposite, J. Mater. Sci. 43 (2008) 4503–4511.
[17] R. Sutton, S. Huo, G. Schaffer, Effect of particle size ratio and particle clustering on sintering and stiffness of aluminium matrix composite, Powder Metall. 49 (2006) 323–327.

[18] N. Chawla, Y.-L. Shen, Mechanical behavior of particle reinforced metal matrix composites, Adv. Eng. Mater. 3 (2001) 357–370.
[19] M.K. Habibi, H. Pouriayevali, M. Gupta, Effect of strain rate and ball milling of reinforcement on the compressive response of magnesium composites, Composites Part A: Appl. Sci. Manuf. 42 (2011) 1920–1929.
[20] M. Gupta, M. Lai, D. Saravanaranganathan, Synthesis, microstructure and properties characterization of disintegrated melt deposited Mg/SiC composites, J. Mater. Sci. 35 (2000) 2155–2165.
[21] G. Garćes, M. RODŔIGUEZ, P. Pérez, P. Adeva, Effect of volume fraction and particle size on the microstructure and plastic deformation of Mg–Y_2O_3 composites, Mater. Sci. Eng. A 419 (2006) 357–364.
[22] S. Sankaranarayanan, S. Jayalakshmi, M. Gupta, Effect of addition of mutually soluble and insoluble metallic elements on the microstructure, tensile and compressive properties of pure magnesium, Mater. Sci. Eng.: A 530 (2011) 149–160.
[23] D. Towle, C. Friend, Comparison of compressive and tensile properties of magnesium based metal matrix composites, Mater. Sci. Technol. 9 (1993) 35–41.
[24] R. Gehrmann, M.M. Frommert, G. Gottstein, Texture effects on plastic deformation of magnesium, Mater. Sci. Eng.: A 395 (2005) 338–349.
[25] G.E. Dieter, Mechanical Metallurgy, McGraw-Hill, New York, 1976.
[26] C.J. Smithells, Metals reference handbook (1955).
[27] M. Sui, K. Lu, Thermal expansion behavior of nanocrystalline Ni–P alloys of different grain sizes, Nanostruct. Mater. 6 (1995) 651–654.
[28] M. Kubisztal, J. Kubisztal, A. Chrobak, G. Haneczok, Young's modulus and adhesion coefficient of amorphous Ni–P coatings on a metal substrate, J. Adhesion Sci. Technol. 21 (2007) 1009–1019.
[29] W.D. Callister, D.G. Rethwisch, Materials science and engineering: an introduction (2007).
[30] D. Lloyd, Aspects of fracture in particulate reinforced metal matrix composites, Acta Metallurgica et materialia 39 (1991) 59–71.
[31] T. Tszeng, The effects of particle clustering on the mechanical behavior of particle reinforced composites, Composites Part B: Eng. 29 (1998) 299–308.
[32] K. Tohgo, G. Weng, A progressive damage mechanics in particle-reinforced metal-matrix composites under high triaxial tension, J. Eng. Mater. Technol. 116 (1994) 414–420.